2nd International Conference on System-Integrated Intelligence: Challenges for Product and Production Engineering

Hardware-accelerated wireless sensor network for distributed Structural Health Monitoring

A. Engel[a]*, A. Friedmann[b], M. Koch[b], J. Rohlfing[c], T. Siebel[b], D. Mayer[b], A. Koch[a]

[a]*Embedded Systems & Applications Group, Computer Science Institute, Technical University Darmstadt, 64289 Darmstadt, Germany*
[b]*Research Division Smart Structures, Fraunhofer LBF, 64289 Darmstadt, Germany*
[c]*System Reliability and Machine Acoustics Group, Technische Universität Darmstadt, 64289 Darmstadt, Germany*

Abstract

Civil infrastructure objects are subject to safety-related issues such as increasing loads and extended service live. Costly manual inspections of these structures should therefore be supplemented by automated continuous monitoring. In this work, a hardware-accelerated wireless sensor network built entirely with energy-efficient embedded components is proposed as the basis for a distributed structural health monitoring (SHM) implementation. In addition to detection and localization of structural damage, the energy-efficiency of the wireless data acquisition system is the major topic of this work. By utilizing the Random-Decrement (RD) technique, the structure's modal parameters are acquired based on ambient excitation such as wind or traffic. The RD functions are calculated by a Field-Programmable Gate Arrays (FPGA) designed for mobile applications. To demonstrate the benefits of the proposed monitoring network, the model of a truss bridge is excited by a train set to simulate realistic operational excitations. Dominant mode shapes of the bridge model are extracted from the RD functions using frequency domain Operational Modal Analysis and compared to previously determined reference measurements. The loosening of a single bolted joint simulates damage and is found to be reflected in significant deviations of the first vertical bending mode, located at 68 Hz.

Keywords: Structural Health Monitoring; operational modal analysis; Wireless Sensor Network; reconfigurable computing

* Corresponding author. Tel.: +49 (6151) 16 - 70974 ; fax: +49 (6151) 16 - 5472.
  E-mail address: engel@esa.cs.tu-darmstadt.de

1. Introduction

Structural health monitoring (SHM) is known as the process of in-service damage detection for aerospace, civil, and mechanical engineering objects and is a key element of strategies for condition based maintenance and damage prognosis [1]. Vibration based damage detection methods have been proven as especially well-suited for the monitoring of large infrastructure objects like buildings, bridges or wind turbines. Most of the methods incorporate the identification of structural dynamic characteristics from vibration measurements and have been tested in the laboratory as well as with actual structures for many years [2].
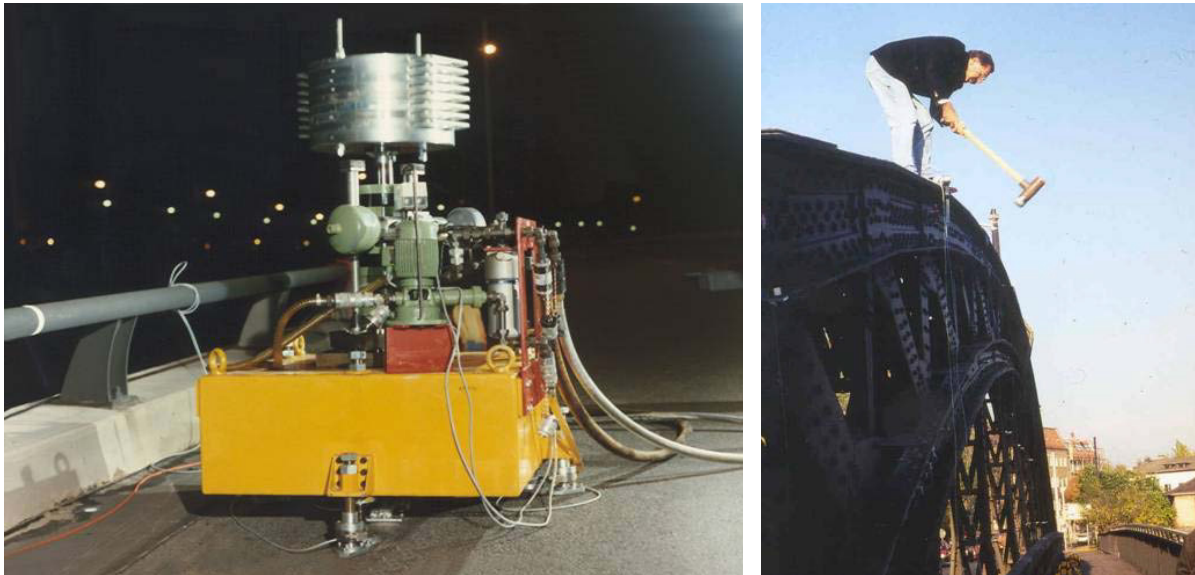

Fig. 1. Exciting bridges with a hydraulic actuator and a mass (left) or using an impact hammer (right) [27].

Most of the structures which are interesting for SHM cannot be excited for structural analysis, either because they are too large (e.g. infrastructure objects) or because it is impractical to apply a vibration exciter during operation (see Figure 1). Thus only the output signals, i.e. the vibrations excited by operational loads can be used in order to estimate the systems behavior. In [3], the Random Decrement (RD) method is evaluated with respect to distributed signal processing on sensor nodes. It is a simple, yet effective method for the estimation of correlation functions [4] and was originally invented for the damage detection of aerospace structures under random loading [5]. The RD technique is also used for data aggregation in the wireless sensor network. Instead of transmitting the sampled acceleration data entirely to a base station for subsequent analysis, the RD functions are computed by the sensor nodes and transmitted to the base station after a certain aggregation time. This significantly reduces the sensor node's communication demands and thus their energy requirements.

The RD technique is a simple method that averages time data series $x(t_n)$ measured on the system under random input loads when a given trigger condition is fulfilled (see Equation 1 as example for a level crossing trigger of trigger level a). The result of this averaging process is called a Random Decrement Signature $D_{XX}(\tau)$.

$$D_{XX}(\tau) = \frac{1}{N} \sum_{n=1}^{N} x(t_n + \tau) \Big| x(t_n) = a \tag{1}$$

The method can be explained descriptively in the following way: At each time instant, the response of the system is composed of three parts: The response to an initial displacement, the response to an initial velocity and the response to the random input loads during the time span between the initial state and the regarded time instant [6]. By averaging many of those time series, the random part will disappear, while the result can be interpreted as the

systems response to the initial condition defined by the trigger, thus, containing information about the systems behavior.

The concept may be extended from auto-correlation functions as described above to the estimation of cross-correlation functions between two system outputs. This is simply achieved by averaging time blocks from one system output (here y) while the averaging process is triggered by another output (here x). If a simple level crossing trigger is assumed, the mathematical expression of the RD technique reads [7]:

$$D_{YX}(\tau) = \frac{1}{N} \sum_{n=1}^{N} y(t_n + \tau) \Big| x(t_n) = a \qquad (2)$$

To estimate the cross-correlation function in a distributed network, the information about trigger events has to be exchanged between the sensor nodes.

The main contribution of this work is the implementation of an automated damage detection application based on the wirelessly distributed data aggregation using hardware-accelerated Random Decrement Technique and a centralized Operational Modal Analysis with subsequent mode shape assessment. This application is evaluated and demonstrated on a model of a truss bridge excited by a railway model.

The remainder of this paper is organized as follows. Section 2 provides an overview about embedded implementations of the Random Decrement Technique. Section 3 describes the setup of the demonstrator. Section 4 details the high level communication protocol of the proposed wireless sensor network (WSN) while Section 5 describes the low level implementation of the hardware-accelerated RD technique. In Section 6, the Operational Modal Analysis and the subsequent damage detection is described. Section 7 provides an experiment evaluation of the proposed monitoring application and Section 8 concludes this work.

2. Related Work

The monitoring of large structures using wireless sensors is the subject of many current research efforts [8] [9] [10] [11]. As an example of a concrete algorithm for such structural health monitoring, the RD technique is used to extract the modal parameters of a monitored structure [7] [12] [13].

Commercially available wireless sensor nodes are often based on low-power microcontrollers (MCUs) aiming for the lowest quiescent current [14]. Zimmermann et al. proposed an RD implementation on such a platform using an 8 bit Atmel MCU and recognized the necessity to improve the energy efficiency of even that low-power system [13].

Reconfigurable compute units (RCU) using Field-Programmable Gate Arrays (FPGAs) can perform complex computations more efficiently then MCUs and digital signal processors (DSP) [15]. In time-critical applications, the use of RCUs often permits computations that cannot be performed by MCUs or Digital Signal Processors (DSPs) at all under the given constraints. FPGAs have thus been employed for mid- to high-performance computing applications, recent work includes [16] [17] [18]. However, all of these studies utilized FPGAs relying on static memory (SRAM) for their configuration storage. While flexible, the use of SRAM precludes the use of deep-sleep modes powering down most of the device (which would lose the configuration information).

For low-power applications, FPGAs using the inherently non-volatile Flash memory are more suitable [19]. To this end, Vera-Salas et al. [20] combined a Flash-based Microsemi Igloo nano FPGA with a wireless transceiver. However, despite the power advantages of Flash configuration storage, this architecture is still sub-optimal in that the FPGA cannot enter device-wide deep sleep since it has to continue to perform low-intensity management tasks such as time-keeping and -synchronization.

The Hardware-Accelerated Low Energy Wireless Embedded Sensor Node (HaLOEWEn) [21] avoids this problem by combining a Flash-based FPGA not only with a wireless transceiver, but with a complete radio system-on-chip (RF-SoC) that also encompasses a low-power processor core. This core has sufficient performance to handle low-intensity administrative tasks, even when the RCU is sleeping.
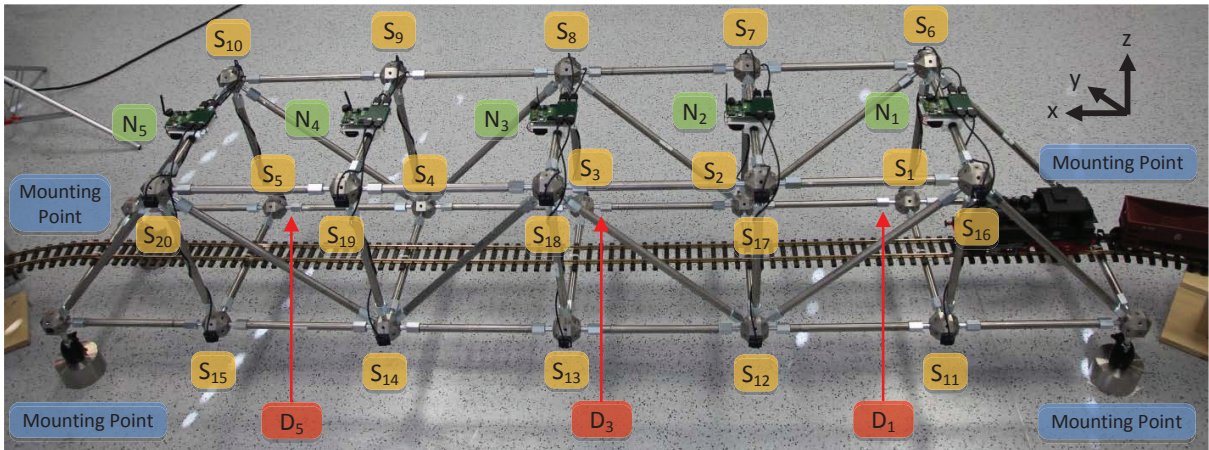
Fig. 2. Bridge model and positions of sensors and sensor nodes.

3. Demonstrator Setup

To demonstrate the proposed damage detection application, a warren truss railroad bridge was modeled by connecting 54 metal rods with 24 metal joints as shown in Figure 2. The bridge model measures 41 cm in y- and z-direction and 246 cm in x-direction. It weighs 51.4 kg and is mounted at its four outer joints allowing its mounting points to rotate but not to move. To simulate damage of the structure screwed connections between rods and joints can be loosened. The three nuts marked as D_1, D_3 and D_5 in Figure 2 were chosen as exemplary damage positions.

A G-scale railway model crossing the bridge is used to generate ambient excitations. The train set has a weight of 2.3 kg and a speed of up to 86 cm/s resulting in 6 bridge crossings per minute.
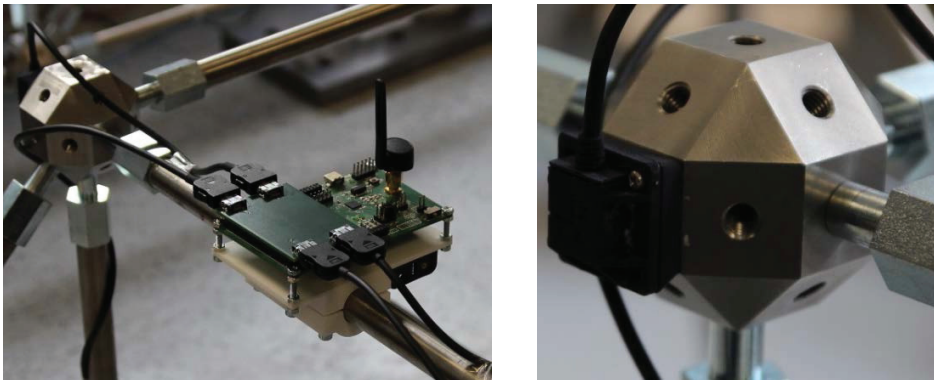

Fig. 3. Mounting of sensors node (left) and sensors (right).

Five battery-powered hardware-accelerated sensor nodes (N_1 to N_5) are mounted on the upper rods of the bridge, as shown in Figure 3. 20 ADXL362 acceleration sensors (S_1 to S_{20}) are mounted at the inner joints of the bridge. These digital MEMS sensors provide a dynamic range of ±2 g at 12 bit resolution and were chosen due to their low dynamic power draw of 6 µW. To ensure a proper transfer of the structural vibration to the acceleration sensors, the ADXL362-breakout boards are sealed in additive manufactured cases, which are screwed to the bridge joints (see Figure 3). Each sensor node controls four acceleration sensors sampling acceleration in the z-direction at 400 Hz.

An additional wireless transceiver (not shown in the graphics) is used as gateway between an embedded PC and the data acquisition network. All sensor nodes are located within the one-hop communication range of the gateway.

4. Wireless Communication

The wireless sensor nodes and the gateway node utilize a TI CC2531 RF-SoC to communicate wirelessly at 2.4 GHz based on the IEEE 802.15.4 MAC protocol. To reduce the packet-overhead to 17 byte per packet (including preamble, control fields, sequence number, addressing and checksums), measurement data and control information are transmitted as MAC payload without an additional network layer header (e.g. Zigbee).
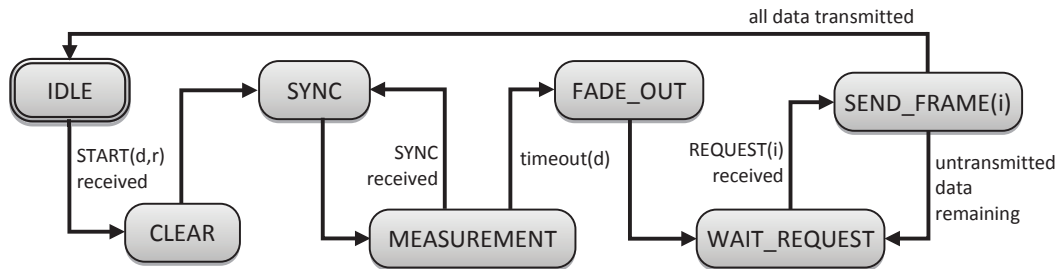

Fig. 4. High level schedule of wirelessly distributed data acquisition.

The high level schedule of the distributed data acquisition phase is initiated and controlled by the gateway as shown in Figure 4. After startup, all sensor nodes are waiting for a *START* packet broadcast by the gateway. This packet includes information on the fixed measurement duration d, during which RD signatures should be accumulated, and the reference configuration $r = (id, a)^n$ specifying the sensor id and the trigger level a of $n \leq 3$ reference signals.

After reception of the *START* packet, all sensor nodes initialize their measurement variables (e.g., clearing all accumulators) and configure their attached hardware accelerator according to the received reference signal selection (see Section 5). Afterwards, they synchronize their local timers to the reception time of the *START* packet. As the CC2531 RF-SoC generates timestamps upon packet reception without the need for software interrupts, the reception times of packages broadcast by the gateway are well defined synchronization points made uncertain only by the distance dependent radio propagation delay (about 3 ns/m). The latter is negligible for the short communication ranges provided by the RF-SoC.

After synchronization, the sensor nodes start sampling their attached sensors at a sampling rate of 400 Hz. In each sampling cycle of the measurement phase, the sensor nodes sampling reference signals x query their attached hardware accelerator, if a trigger event was registered. If a trigger event was registered in sampling cycle t_n, all other sensor nodes have to be informed about this event to enable the calculation of the cross-correlation signatures D_{YX} (see Equation 2). However, registered trigger events are not broadcast immediately, as transmitting a single byte of information would result in a large packet overhead (93 %) thus poorly utilizing the energy required for the wireless transmission. Furthermore, the generation of trigger events at the different reference signals is highly correlated in time and place, i.e. nearby reference signals will also register a trigger event in the same sampling cycle with a high probability. Therefore, immediate broadcasting of registered trigger events would lead to channel congestion and must be resolved (e.g., by CSMA-CA). Finally, potential trigger event broadcasting in every sampling cycle requires all nodes to listen for incoming packages in every sampling cycle. As listening to the radio channel requires about the same power as transmitting data, the system energy requirements would increase dramatically.

These problems (low packet utilization, channel congestion and idle listening) can be met by explicitly delaying the trigger event broadcasts until some predefined sampling cycle reserved for the particular reference signal. The proposed scheduling scheme used in the current implementation is shown in Table 1. Every hundredth sampling cycle is actually reserved for communication and the radio transceivers can thus be turned off 99 % of the time. Besides the three potential transmitters of trigger events, a fourth slot is reserved for the gateway transmitting synchronization packets. These are required to resynchronize all sensor nodes to a common time base as the local timers run at slightly different speeds (temperature dependent drifts of a few ppm) thus drifting apart with a few µs/s. Currently, the gateway transmits one *SYNC* packet per second, thus utilizing all of its reserved slots.

Table 1. Radio transmitter scheduling.

Sampling cycle	01	...	99	100	101	...	199	200	201	...	299	300	301	...	399	400	401	...	499	500	...	599	600	601	...
TX REFERENCE 1				▓																▓					
TX REFERENCE 2								▓															▓		
TX REFERENCE 3												▓													
TX GATEWAY																▓									

The trigger events of each reference signal can be broadcast every 400 sampling cycles. If less than 25 trigger events have to be transmitted, each event is represented by a 16 bit offset relative to the broadcast cycle. For 25 trigger events and above, a 400 bit map is used to represent the sampling cycles in which trigger events where generated. Both cases can be distinguished at the receiver by the payload size. Furthermore, no additional information is required to represent the index of the trigger generating reference signal, as this is implicitly given by the time of the broadcast. Thus, the maximum payload length during measurement is 50 Bytes. Together with the 17 byte packet overhead, the transmission and reception of such a packet takes 2144 µs (86 % of a sampling period). As the computationally intense data aggregation is done in parallel by the hardware accelerator, transceiving those large packages does not interfere with the real time execution at the RF-SoC.

At the end of the measurement (determined by the duration send with the *START* packet), a fade out phase is required to ensure proper handling of trigger events registered but not completely handled. Within this phase, no new triggers events are generated, but the sensor nodes keep sampling their sensors until the buffers managed by the hardware accelerators are emptied.

After data aggregation, the results, comprising up to 12 RD signatures and additional statistics like the variance of each sensor signal and the number of trigger events handled by each sensor node, have to be transmitted to the gateway. The gateway has to forward the received data to the embedded PC through a serial communication link with a data rate smaller than the wireless communication rate. To avoid buffer overflows at the gateway, the data set to be transmitted is sliced into 112 byte frames and each frame from each sensor node is explicitly requested by the gateway. Overdue frames are re-requested after a fixed timeout to handle packet loss. After transmission of the last frame, the sensor nodes return to the idle state waiting for the start of the next measurement.

5. Hardware-Accelerated Random Decrement Technique

A Microsemi IGLOO AGL1000V2 FPGA is used as hardware accelerator of the HaLOEWEn sensor node [15]. The communication between the RF-SoC and the hardware accelerator is based on a hardware kernel API described in [22]. The signal processing chain required to calculate an RD signature is shown in Figure 5. An SPI controller provides the sampled values of a signal y, which are passed through a high-pass filter (HPF) to eliminate static acceleration (gravity). The filtered signal is compared against the trigger level configured for signal y and passed to a variance calculator. Furthermore, the filtered signal is delayed by 400 sampling cycles through a FIFO, before it may be accumulated to the RD signature D_{YX}. The position within the RD signature to accumulate the FIFO output to is determined by the set of triggers events generated for signal x. The FIFO output may be accumulated to multiple positions within D_{YX} if the delay between subsequent trigger events is shorter than the RD signature.

With four attached sensors and up to three reference signals, up to 12 RD signatures have to be calculated by the hardware accelerator at each sensor node. However, most of the computing elements described in Figure 5 can be shared by multiple RD signatures, as shown in Figure 6. All of these blocks can be executed in parallel thus
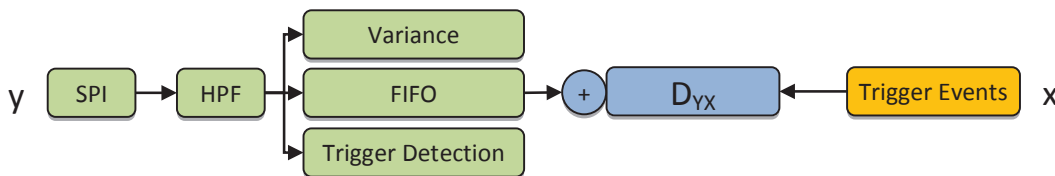

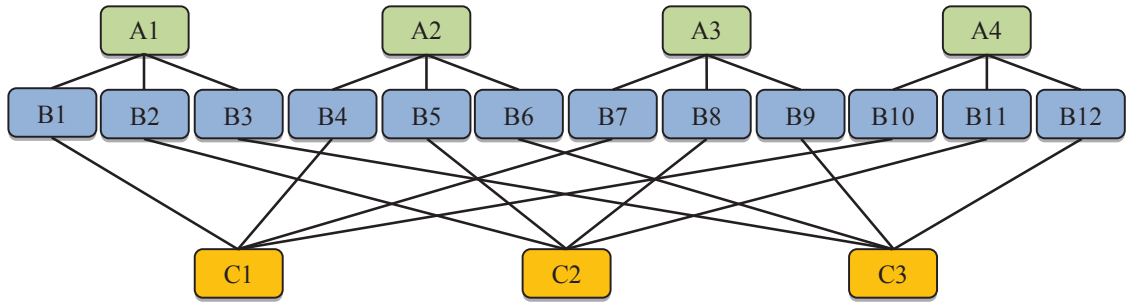Fig. 5. Signal processing chain for a single RD signature.

Fig. 6. Resource-sharing for computing multiple RD signatures.

restricting the execution time of the hardware accelerator to 32 clock cycles for the SPI communication + 33 clock cycles for the high-pass filter (realized as sequential FIR filter of order 32) + one clock cycle for the FIFO (implemented as circular buffer).

6. Operational Modal Analysis and Damage Detection

Asmussen [7] proved that a connection between RD signatures D_{YX} and correlation functions R_{YX} can be established. For a level crossing trigger condition, the factors used to derive correlation functions from RD signatures are the trigger level a itself and the variance σ_X^2 of the triggered signal to

$$R_{YX}(\tau) = D_{YX}(\tau)\frac{\sigma_X^2}{a} \tag{3}$$

The matrices R of the correlation functions are evaluated by a Matlab routine on the embedded PC. Having read all correlation functions of the matrix R, an intermediate step is needed before starting with the modal decomposition. Because the algorithms of frequency domain based operational modal analysis need a matrix $G(f)$ of spectral densities as an input, a single block DFT has to be applied to the correlation functions [23]. It should be mentioned that within this DFT, no use is made of time windowing. For the subsequent Operational Modal Analysis, the FDD algorithm is used. This algorithm described first by Brincker et. al. [24] is based on a Singular Value Decomposition of the matrix $G(f)$. For every frequency f, this process leads to two fully populated matrices $U(f)$ and a diagonal matrix $S(f)$ holding the spectra of the so-called singular values $S_{ii}(f)$ in decreasing order:

$$(f) = U(f) \cdot S(f) \cdot U^H(f) \tag{4}$$

The peak values of the first singular values then are interpreted as indicators for the system eigenfrequencies. Furthermore, with the FDD algorithm it is possible to estimate the mode shapes for the found frequencies. The eigenvectors describing the mode shapes connected to the eigenfrequencies determined by the first singular values can be found in the first column of the matrix $U(f)$.

A damage index (DI) based on normalized mode shapes is applied for damage localization. The procedure is derived from the Modal Strain Energy method (MSE) [25]. However, the MSE relies on mode shape curvatures, which can hardly be derived with sufficient precision from experimental, eventually noisy data [26]. Thus, in the applied approach, instead of analyzing the curvature, the displacement ϕ_{S_i} of sensor S_i in the first vertical bending mode is normalized according to

$$F_{S_i} = \frac{\phi_{S_i}^2}{\sum_{k=1}^{20} \phi_{S_k}^2} \qquad 1 \le i \le 20. \tag{5}$$

The DI for each sensor S_i describes the relative deviation of the measured mode shape from a reference mode shape ($\hat{F}$) as

$$DI_{S_i} = \frac{F_{S_i}+1}{\hat{F}_{S_i}+1} - 1 \qquad 1 \leq i \leq 20. \tag{6}$$

To locate the damage along the x-direction of the bridge model, the DI of all sensors with the same x-coordinate are accumulated to

$$DI_x = \sum_{k=0}^{3} DI_{S_{5k+x}} \qquad 1 \leq x \leq 5. \tag{7}$$

7. Experimental Evaluation

Table 2. Demonstrator configuration for evaluation.

sensor nodes	5	Sampling rate	400 Hz
signals per sensor node	4	Synchronization rate	1 Hz
Max. number of reference signals	3	Length of RD signature	640 ms
Signal / Triggerlevel for Reference 1	S_3 / 200 mg	Depth of RD signature	24 bit / sample
Signal / Triggerlevel for Reference 2	S_{13} / 200 mg	Max. measurement duration	3600 s
Signal / Triggerlevel for Reference 3	Not used		

The demonstrator configuration used for evaluation is summarized in Table 2. With these settings, the FPGA utilizes 75 % of its logic elements, 81 % of its storage elements and may be driven at a clock rate of 11 MHz. However, the ADXL362 restricts its serial clock to 1 MHz and for simplicity this clock rate is used for the entire FPGA logic. The resulting execution time of the hardware accelerator is 66 µs or 2.6 % of the sampling period respectively. At this duty cycle, the simulated power consumption of the hardware accelerator amounts to 112 µW (2.2 mW active, 54 µW sleep).

The power drawn by the RF-SoC during measurement heavily depends on the number of actually transmitted packets and thus on the excitation of the monitored structure. An upper bound can be derived as follows. To control the hardware accelerator without any radio communication, the RF-SoC requires 69 µs or 2.8 % of the sampling period. This duty cycle results in a base load of 558 µW (20 mW active, 6 µW sleep). In 1 % of the sampling cycles, the radio transceiver may occupy up to 86 % of the sampling period. The activated transceiver consumes about 70 mW thus raising the RF-SoCs power budget by up to 602 µW. Taking into account the additional power consumers (sensors, oscillators, DC/DC converters), the sensor nodes will not draw more than 2 mW from their power supply. In comparison, the pure transmission costs for sending four 12 bit sensor samples over the 250 kbit/s radio channel would last 192 µs or 7.68 % of each sampling cycle resulting in 5.4 mW power draw of the radio transceiver, when neglecting idle power and packet overhead. Therefore, our proposed decentralized data aggregation network will not consume more than a third of the energy required by a centralized wireless data acquisition network.
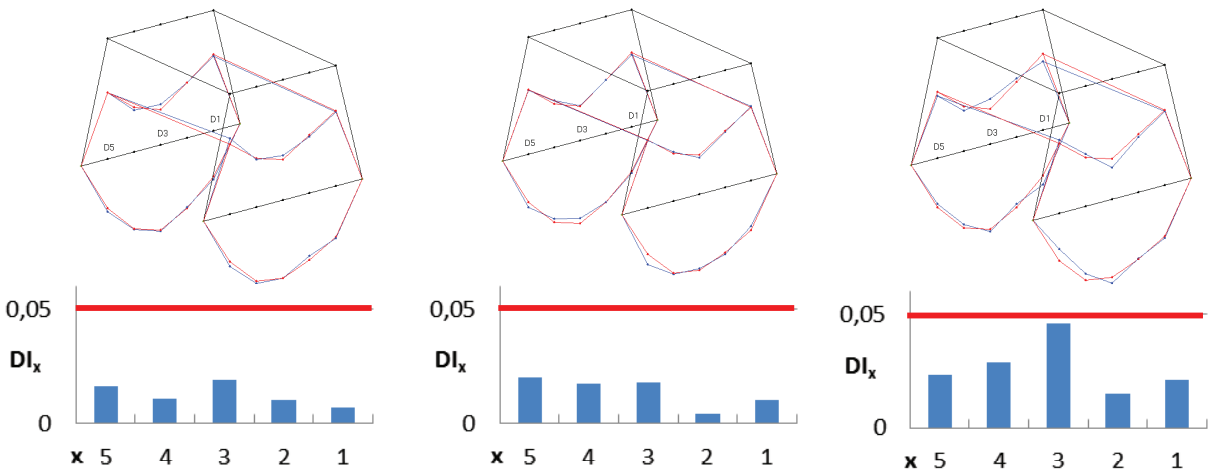

Fig. 7. Mode-shapes and DI_x of undamaged structure obtained from 300 s (left), 60 s (center) and 30 s (right) measurements.

For the selected configuration of the reference signals, each bridge crossing of the train generates 12 to 20 trigger events at each reference signal. The reference mode shape of the bridge was derived from a 10 minute measurement, which generated 1103 triggers events at S_3 and 873 trigger events at S_{13}.

To demonstrate the reproducibility of the mode shape determined for the undamaged structure, measurements of reduced duration have been carried out. The resulting mode shapes of the first vertical bending mode located at 68 Hz and the corresponding damage indexes are shown in Figure 7. The reference mode shape is shown in red, while the actually determined mode shape is shown in blue. The number of accumulations performed for each RD signature decreases with the measurement duration and the remaining noise in the RD signatures results into larger DI values. The possibility of false positive damage detection thus increases. For the experimentally determined damage detection threshold of 0.05, a 60 s measurement interval provides sufficiently low DI values.

Figure 8 shows the mode shapes and the damage indexes determined from the damaged structure for the 3 different damage locations detailed in Figure 2. In all three cases, the damage has been detected. The damage location is roughly reflected by the DI diagram, but the exact position of the loosened nut can not be determined.
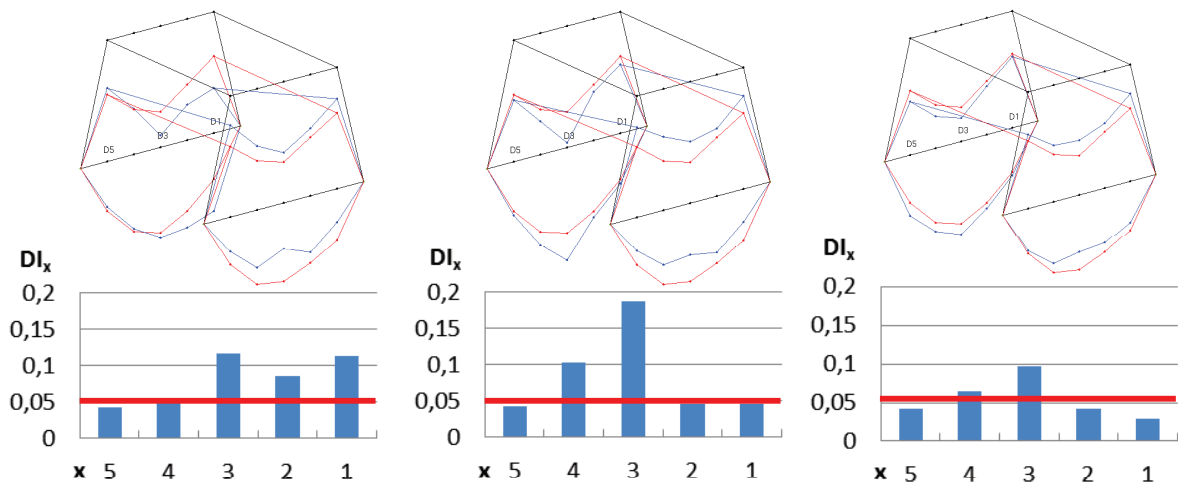

Fig. 8. Mode-shapes and DI_x of damaged structure obtained from a 300 s measurement after loosening D_1 (left), D_3 (center) or D_5 (right) by a 5/6 rotation.

8. Conclusion

An automated damage detection algorithm relying on the wirelessly distributed estimation of cross-correlation functions and an operational modal analysis was implemented and evaluated on an ambient excited model of a railway bridge. The Random Decrement technique was implemented by the hardware-accelerator of the HaLOEWEn sensor node efficiently exploiting parallel signal processing to compute multiple RD signatures. The aggregation of the sensed data reduces the power required by the sensor nodes below 2 mW. The mode shapes of the structure can be determined based on the estimated correlation functions. Damage can be detected automatically but not yet located with sufficient confidence. Future work will thus deal with the optimization of the reference settings and the formulation of the damage index for improved damage localization. Furthermore, robustness issues such as detecting node failures and automatic reorganization of the network must be addressed.

Acknowledgements

References

[1] Friedmann A, Koch M, Mayer D. Using the Random Decrement Method for the Decentralized Acquisition of Modal Data. Proceedings of ISMA2010 including USD2010 2010.

[2] Brincker R, Krenk S, Jensen JL, Estimation Of Correlation Functions By The Random Decrement. Proceedings of The Florence Modal Anaylsis Conference 1991.

[3] Cole HA. On-line failure detection and damping measurement of aerospace structures by random decrement. CR-2205. NASA; 1973.

[4] Rodrigues J, Brincker R. Application of the Random Decrement Technique in Operational Modal Analysis. Proceedings of the 1st International Operational Modal Analysis Conference 2005.

[5] Asmussen JC. Modal Analysis Based on the Random Decrement Technique: application to civil engineering structures. Aalborg: Aalborg University Press; 1998.

[6] Sazonov E, Janoyan K, Jha R. Wireless intelligent sensor network for autonomous structural health monitoring. Smart Structures and Materials 2004: Smart Sensor Technology and Measurement Systems 2004;5384:305-314.

[7] Koch M, Bollenbacher H, Mayer D, Kauba M, Friedmann A. Entwicklung und Umsetzung von verteilten Systemen zur Vibrationsanalyse und Strukturidentifikation. Darmstadt: Fraunhofer LBF; 2009.

[8] Kim S, Pakzad S, Culler D, Demmel J, Fenves G, Glaser S, M Turon. Wireless sensor networks for structural health monitoring. Proceedings of the 4th International Conference on Embedded Networked Sensor Systems 2006.

[9] Pakzad SN , Fenves GL, Kim S, Culler DE. Design and Implementation of Scalable Wireless Sensor Network for Structural Monitoring. Journal of Infrastructure Systems 2008;14:89-101.

[10] Mayer D, Friedmann A, Koch M, Dornbusch T. Realization and Testing of an In-Service Vibration Analysis System for Structural Health Monitoring. Proceedings of the 6th European Workshop on Structural Health Monitoring 2012.

[11] Zimmerman AT , Shiraishi M, Swartz RA, Lynch JP. Automated Modal Parameter Estimation by Parallel Processing within Wireless Monitoring Systems. Journal of Infrastructure Systems 2008;14:102-113.

[12] Bischoff R, Meyer J, Feltrin G. Wireless Sensor Network Platforms. Encyclopedia of Structural Health Monitoring. Hoboken: John Wiley & Sons; 2009.

[13] Engel A, Liebig B, Koch A. Feasibility Analysis of Reconfigurable Computing in Low-Power Wireless Sensor Applications. In: Reconfigurable Computing: Architectures, Tools and Applications. Belfast: Springer; 2011.

[14] Kohvakka M, Arpinen T, Hannikainen M, Hamalainen TD. High-performance multi-radio WSN platform. Proceedings of the 2nd international workshop on Multi-hop ad hoc networks: from theory to reality 2006.

[15] Zhiyong CH, Pan LY, Zeng Z, Meng MQ-H. A novel FPGA-based wireless vision sensor node. Proceedings of the IEEE Int. Conf. Automation and Logistics 2009.

[16] Krasteva Y, Portilla J, de la Torre E, Riesgo T. Embedded Runtime Reconfigurable Nodes for Wireless Sensor Networks Applications. IEEE Sensors Journal 2011;11(9):1800-1810.

[17] Nyländen T, Janhunen J, Hannuksela J, Silven O. FPGA based application specific processing for sensor nodes. Proceedings of the International Conference on Embedded Computer Systems 2011.

[18] Vera-Salas L , Moreno-Tapia S, Osornio-Rios R, de J Romero-Troncoso R. Reconfigurable Node Processing Unit for a Low-Power Wireless Sensor Network. International Conference on Reconfigurable Computing and FPGAs 2010.

[19] Philipp F , Samman F, Glesner M. Design of an autonomous platform for distributed sensing-actuating systems. 22nd IEEE International Symposium on Rapid System Prototyping 2011.

[20] Engel A, Liebig B, Koch A. Energy-efficient heterogeneous reconfigurable sensor node for distributed structural health monitoring. Conference on Design and Architectures for Signal and Image Processing 2012.

[21] McConnell KG. Vibration Testing: Theory and Practice. New York: John Wiley & Sons, Inc.; 1995.

[22] Brincker R, Zhang L, Andersen P. Modal Identification from Ambient Responses using Frequency Domain Decomposition. Proceedings of the International Modal Analysis Conference 18 2000.

[23] Stubbs N, Kim J-T, Farrar CR. Field verification of a nondestructive damage localization and severity estimation algorithm. Proceedings of IMAC XIII 1995.

[24] Siebel T, Friedmann A, Koch M, Mayer D. Assessment of Mode Shape-Based Damage Detection Methods under Real Operational Conditions. Proceedings of the 6th European Workshop on Structural Health Monitoring 2012.

[25] VDI Wissensforum. Bauwerksüberwachung. 2013.

[26] Dornbusch T, Nottbeck M, Bartel T, Buff H, Friedmann A, Kauba M, Koch M, Mayer D. Experimental investigation of a Random Decrement based modals estimation on a pedestrian bridge. Proceedings of the 14th Intternational Adaptronic Congress 2011.